Clustering in Low Density Nuclear Matter

Joseph B. Natowitz,
Department of Chemistry and Cyclotron Institute, Texas A&M University, College Station, Texas 77843, USA

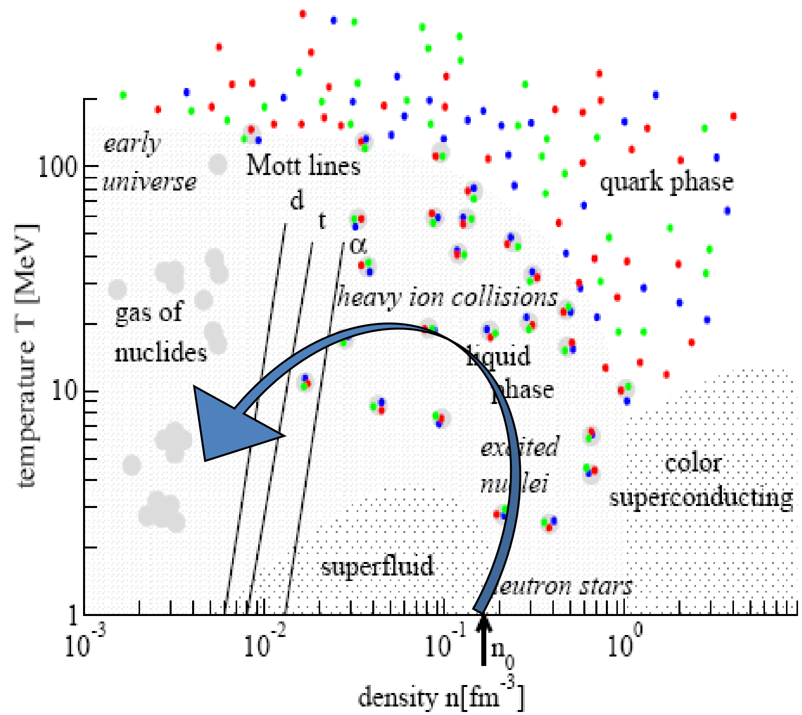

Workshop on Light clusters in nuclei and nuclear matter:
nuclear structure and decay, heavy-ion collisions, and astrophysics
ECT, Trento September 2019

NIMROD- ISiS 4 Pi Charged Particles - 4 Pi Neutrons

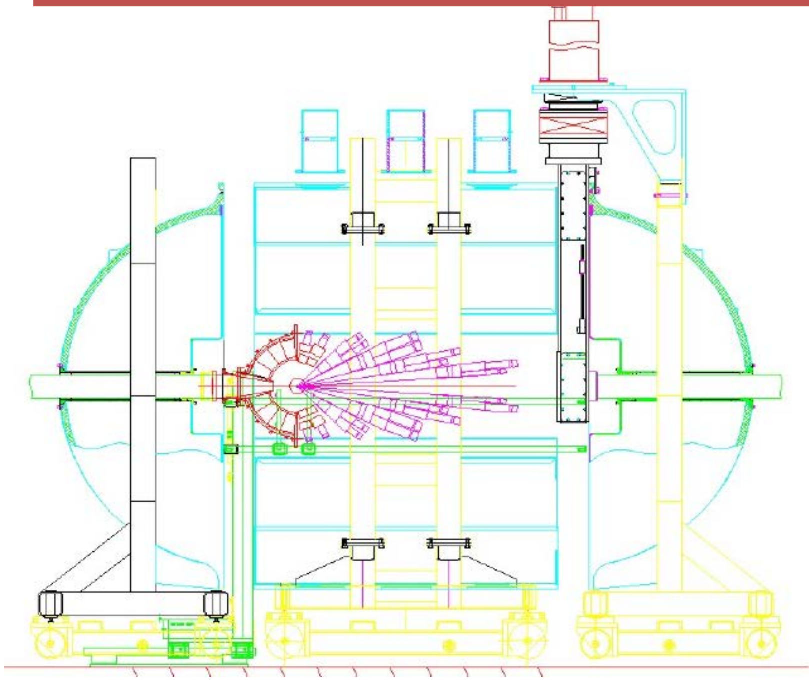

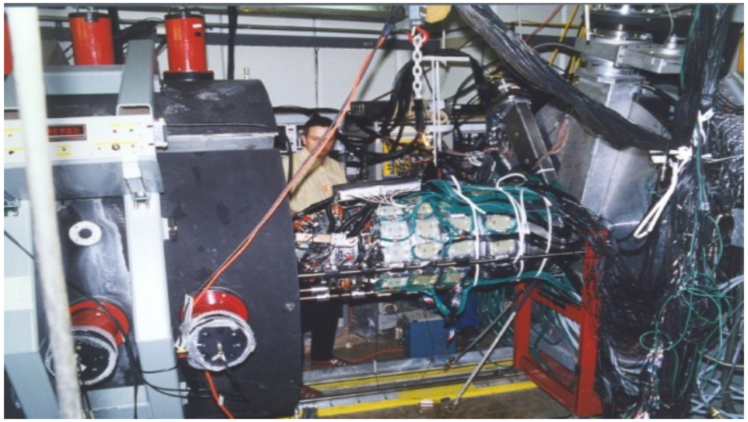

- 14 Concentric Rings
- Silicon-CsI
- 3.6-167 degrees
- Neutron Ball

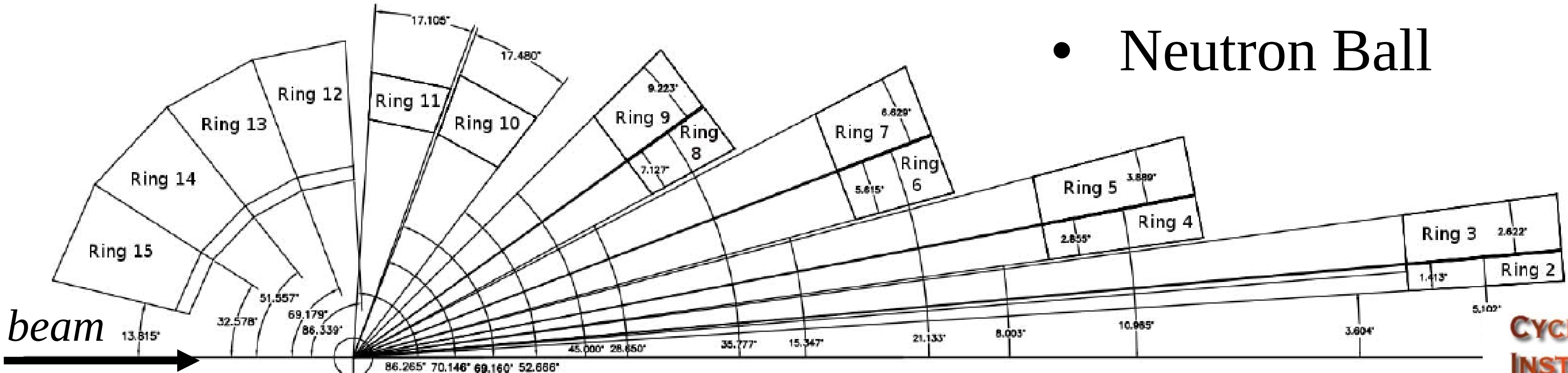

S. Wuenschel et al., Nucl. Instrum. Methods. A604, 578–583 (2009).

Cyclotron Institute
Texas A&M University

PHYSICAL REVIEW C, VOLUME 62, 034607

Light particle probes of expansion and temperature evolution: Coalescence model analyses of heavy ion collisions at 47*A* MeV

K. Hagel,[1] R. Wada,[1] J. Cibor,[1,2] M. Lunardon,[1,3] N. Marie,[1,4] R. Alfaro,[1] W. Shen,[5] B. Xiao,[1] Y. Zhao,[1] Z. Majka,[6] J. Li,[1] P. Staszel,[2] B.-A. Li,[1] M. Murray,[1] T. Keutgen,[1] A. Bonasera,[1,7] and J. B. Natowitz[1]

[1]*Cyclotron Institute, Texas A&M University, College Station, Texas 77843*

[2]*Institute of Nuclear Physics, ul. Radzikowskiego 152, PL-31-342 Krakow, Poland*

[3]*Universita di Padua, Dipartimento di Fisica, Padova, Italy*

[4]*Laboratoire de Physique Corpusculaire, 14050 Caen Cedex, France*

[5]*Chinese Academy of Science, Shanghai Institute of Nuclear Research, Shanghai 201800, People's Republic of China*

[6]*Jagellonian University, M Smoluchowski Institute of Physics, PL-30059 Krakow, Poland*

[7]*Laboratori Nazionali del Sud, I-95123 Catania, Italy*

(Received 29 March 2000; published 14 August 2000)

The reactions $^{12}C+^{116}Sn$, $^{22}Ne+Ag$, $^{40}Ar+^{100}Mo$, and $^{64}Zn+^{89}Y$ have been studied at 47*A* MeV projec-

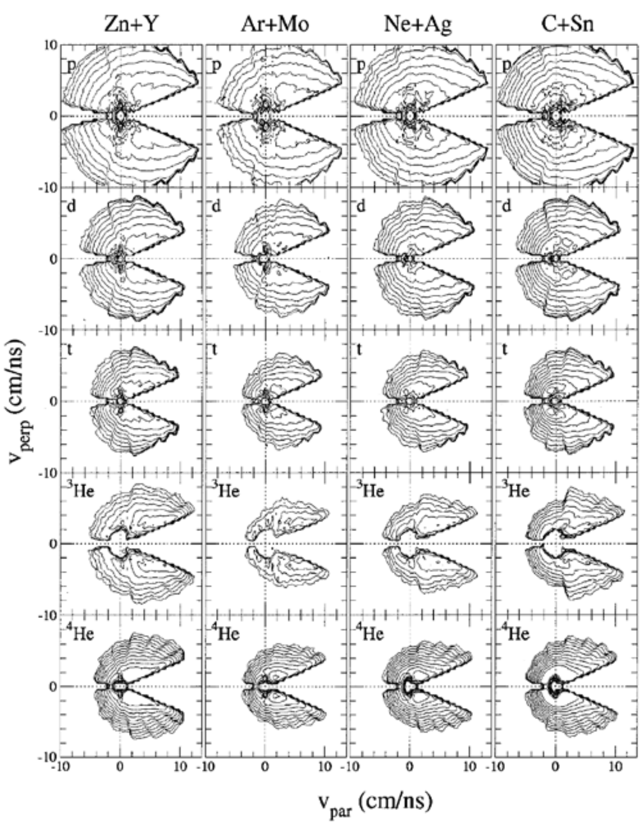

FIG. 5. Invariant velocity plots for *p*, *d*, *t*, ^{3}He, and ^{4}He detected in violent collisions for the reactions $^{12}C+^{116}Sn$, $^{22}Ne+Ag$, $^{40}Ar+^{100}Mo$, and $^{64}Zn+^{89}Y$. Each contour indicates an increase in intensity of a factor of 2.

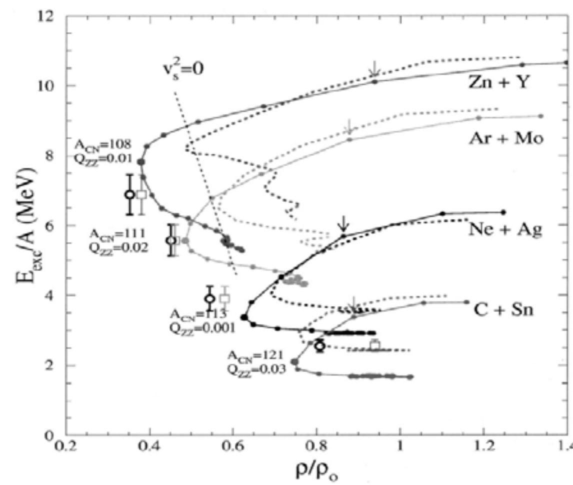

FIG. 20. Excitation energy-density values at freeze-out. The symbols represent the excitation-energy–density values, open circles, Mekjian model, open squares, Sato-Yazaki model, derived from coalescence model analyses of the light cluster emission. They are compared to CHIMERA QMD model trajectories in the excitation energy per nucleon-normalized density plane calculated for central collisions in the four different systems studied. Calculations for a soft $K=200$ MeV, equation of state are represented by solid lines. Calculations for a hard, $K=380$ MeV, equation of state are represented by thick dashed lines. The trajectories start at the time of maximum density. The small dots mark time increments of 10 fm/c. Arrows indicate the time of first emission of particles (near 50 fm/c after contact). Both times and Qzz values are indicated at the minimum calculated densities (large solid dots). To the left of the dashed line $V_s^2=0$, is the spinodal region [18–20].

Velocity Plots

Light Charged Particles- Most Violent Collisions

Velocity Plot Protons
$^{40}Ar+^{124}Sn$

Experiment

V perpendicular

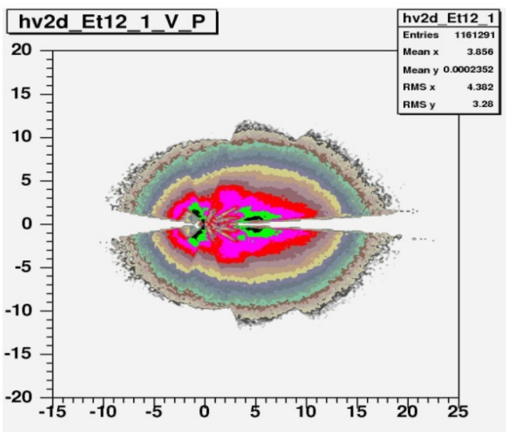

V parallel

From Fitting

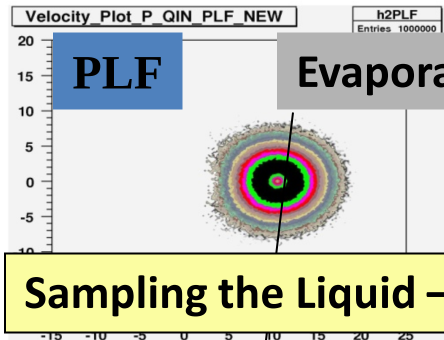

PLF

Evaporation-like

Sampling the Liquid – late emission

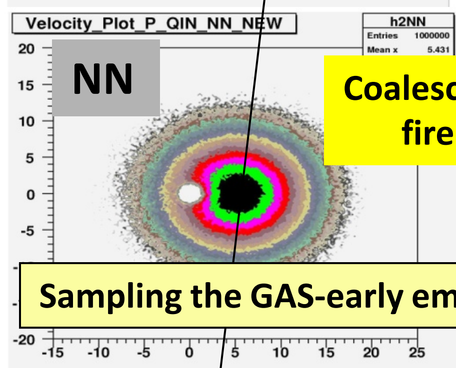

NN

Coalescence-like fireball

Sampling the GAS-early emission faster particles

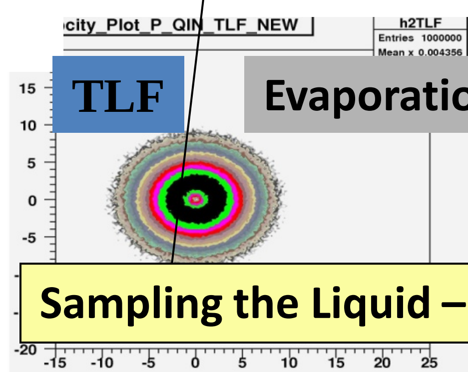

TLF

Evaporation-like

Sampling the Liquid – late emission

Sum of Source Fits

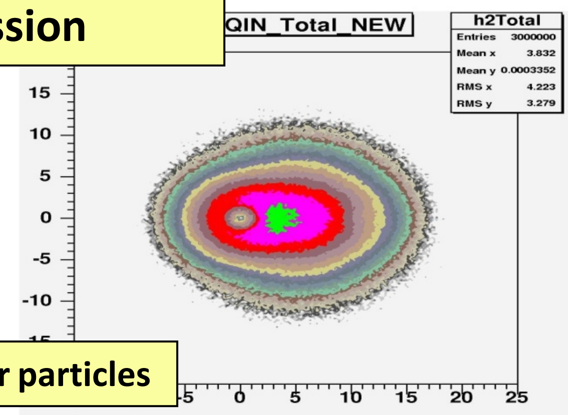

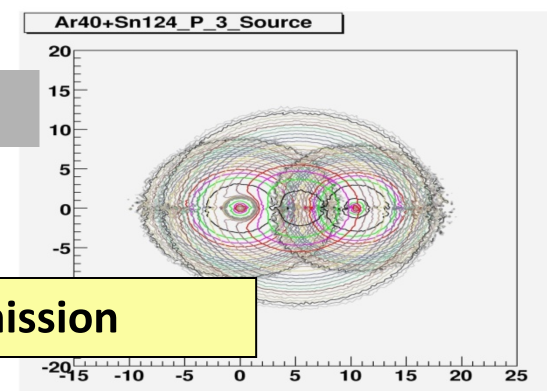

The equilibrium constant of a chemical reaction

$$\alpha A + \beta B ... \rightleftharpoons \rho R + \sigma S ...$$

is the value of the reaction quotient when the reaction has reached equilibrium.

For a general chemical equilibriumthe thermodynamic equilibrium constant can be defined such that, at equilibrium,[1][2]

$$K^\ominus = \frac{\{R\}^\rho \{S\}^\sigma ...}{\{A\}^\alpha \{B\}^\beta ...}$$

where curly brackets denote the thermodynamic activities** of the chemical species. The right-hand side of this equation corresponds to the reaction quotient Q for arbitrary values of the activities. The reaction coefficient becomes the equilibrium constant as shown when the reaction reaches equilibrium.

An equilibrium constant value is independent of the analytical concentrations of the reactant and product species in a mixture, but depends on temperature and on ionic strength. Known equilibrium constant values can be used to determine the composition of a system at equilibrium.

$$\Delta G^\ominus = -RT \ln K^\ominus$$

The equilibrium constant is related to the standard Gibbs free energy change for the reaction.

If deviations from ideal behavior are neglected, the activities of solutes may be replaced by concentrations, [*A*], and the activity quotient becomes a concentration quotient, K_c.

$$K_c = \frac{[R]^\rho [S]^\sigma ...}{[A]^\alpha [B]^\beta ...}$$

K_c is defined in an equivalent way to the thermodynamic equilibrium constant but with concentrations of reactants and products instead of activities. (K_c appears here to have units of concentration raised to some power while K is dimensionless; however the concentration factors in K_c are properly divided by a standard concentration so that K_c is dimensionless also.

** In chemical thermodynamics, **activity**) is a measure of the “effective concentration” of a species in a mixture. The species' chemical potential depends on the activity Activity depends on temperature, pressure and composition of the mixture, among other things. The difference between activity and other measures of composition arises because molecules in non-ideal gases or solutions interact with each other, either to attract or to repel each other.

Equilibrium constants from α-particles model predictions

$$K_c(A,Z) = \frac{\rho(A,Z)}{\rho_p^Z \rho_n^{(A-Z)}}$$

- Many tests of EOS are done using mass fractions and various calculations include various different competing species.
- If any relevant species are not included, mass fractions are not accurate.
- Equilibrium constants are more robust than mass fractions.
- Differences in the equilibrium constants may offer the possibility to study deviations from ideality-interactions between species
- Models converge toward ideality at lowest densities.

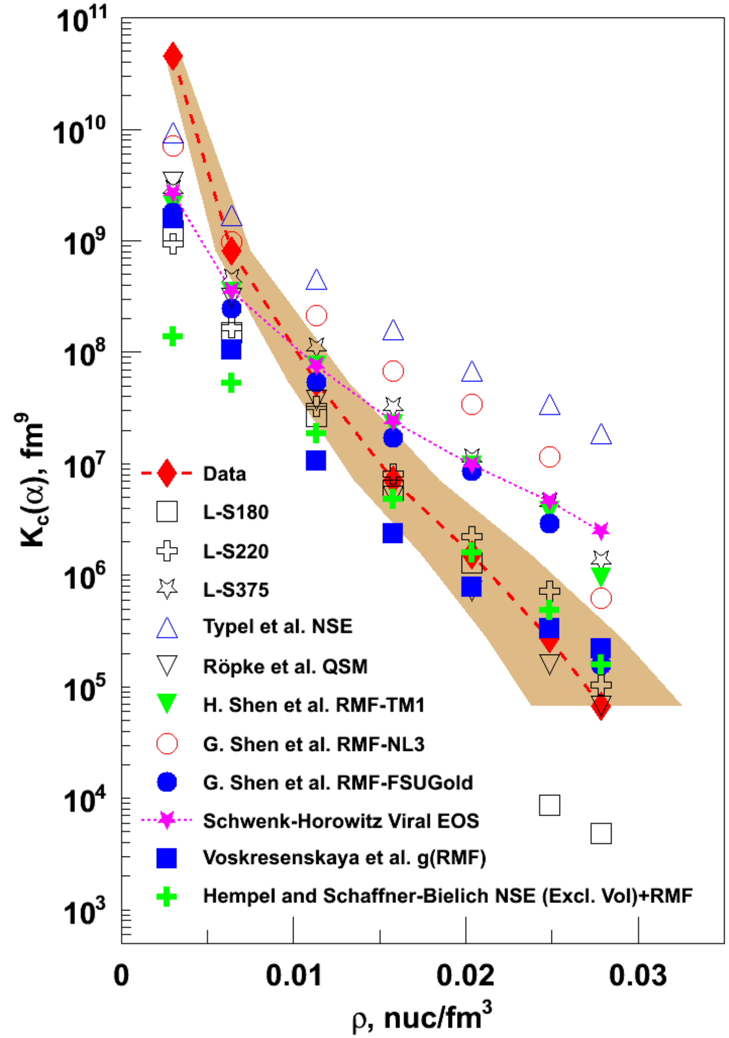

PRL **108** (2012) 172701.

The Symmetry Energy Problem
Density Dependence ?

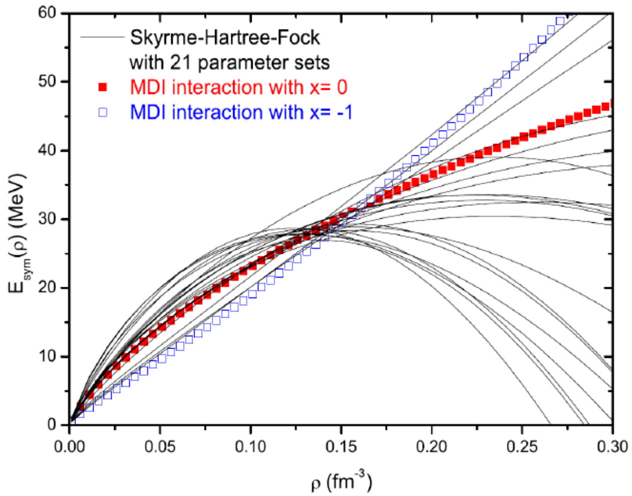

Experimentally or observationally constraining the density dependence of the symmetry energy over a broad range of densities is a complex problem-

E/A

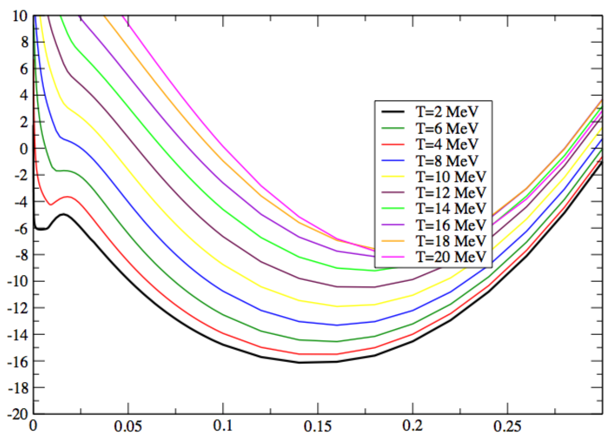

Rho

While low density situation would appear to be easier to constrain- cluster formation changes the medium This leads to additional complexity (opportunity)

SYMMETRY ENERGY LOW DENSITY LIMIT

At Low Density The Symmetry Energy is Determined by Cluster Formation. Analysis of Cluster Yield Ratios For Different N/Z Systems (ISOSCALING) Allows Determination of The Symmetry Free Energy. Employment of Entropies Calculated with the QSM Model of Roepke, Typel et al (shown to be appropriate by other measured quantities) Allows Extraction of The LOW Density Symmetry Energy $F_{sym} + T \cdot S_{sym} = E_{sym}$

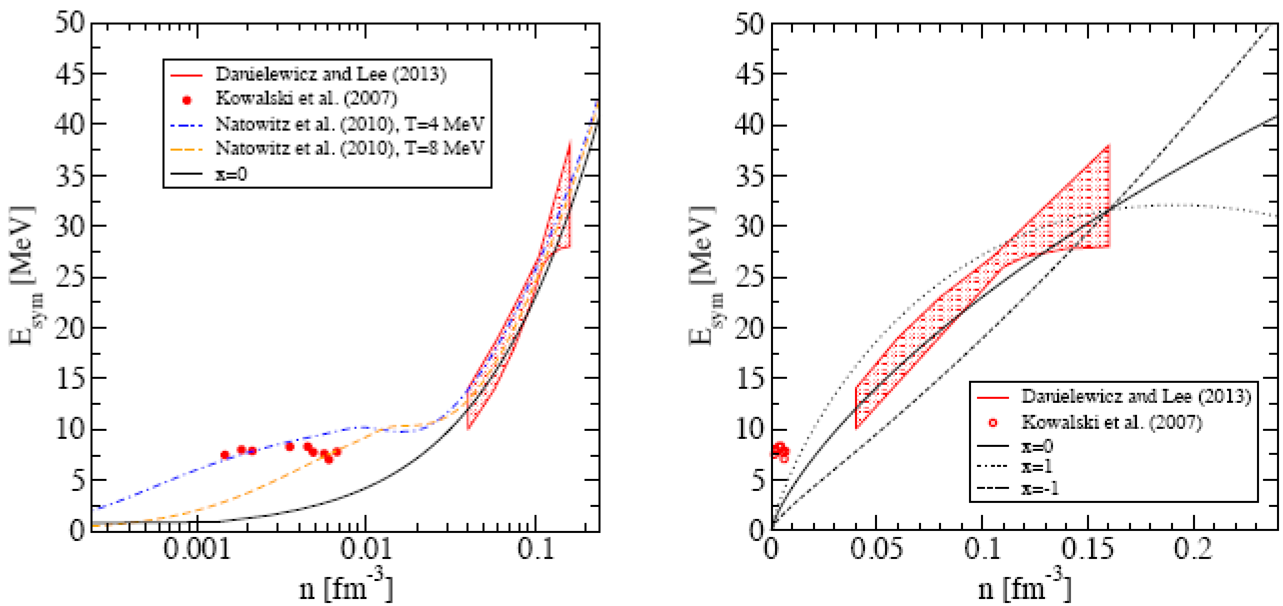

<u>The equation of state and symmetry energy of low density nuclear matter</u>

K. Hagel, G. Roepke and J. Natowitz , EPJA, **50**, 39 (2014)

See also S. Typel *et al*., Phys. Rev. C 81, 015803 (2010).

J.B. Natowitz et al., Phys.Rev.Lett.104:202501 (2010).

NOTE CHEMICAL EQUILIBRIUM ASSUMPTIONS FOR FIREBALL

Density dependent binding energies

- From Albergo, recall that $K_c(A,Z) = \mathrm{C(T)}e^{\left(\frac{B(A,Z)}{T}\right)}$
- Invert to calculate binding energies
- Entropy mixing term $\Delta F = T\left(Z ln\left(\frac{Z}{A}\right) + N ln\left(\frac{N}{A}\right)\right)$

$$ln[K_c/C(T)] = \frac{B}{T} - Z ln\left(\frac{Z}{A}\right) - N ln\left(\frac{N}{A}\right)$$

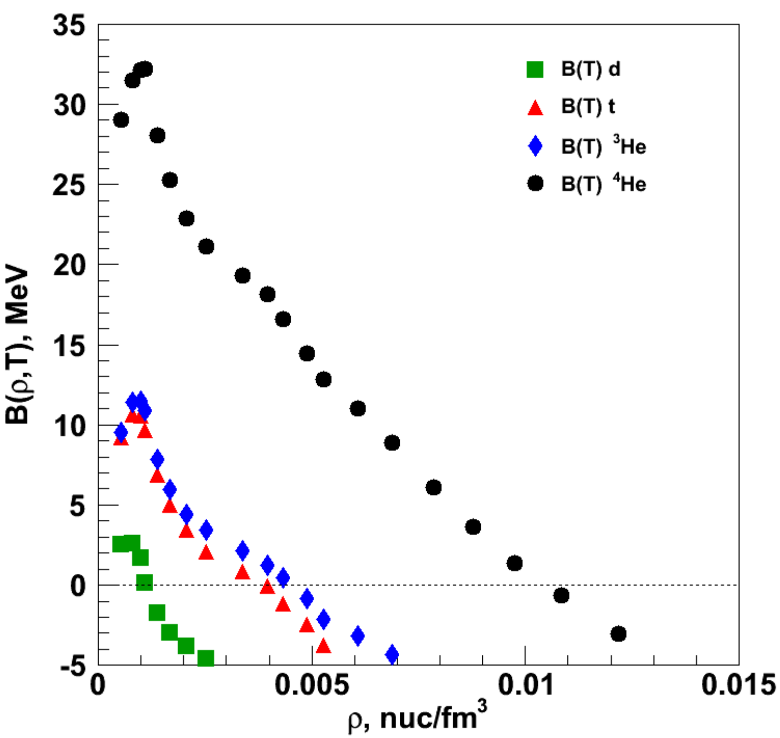

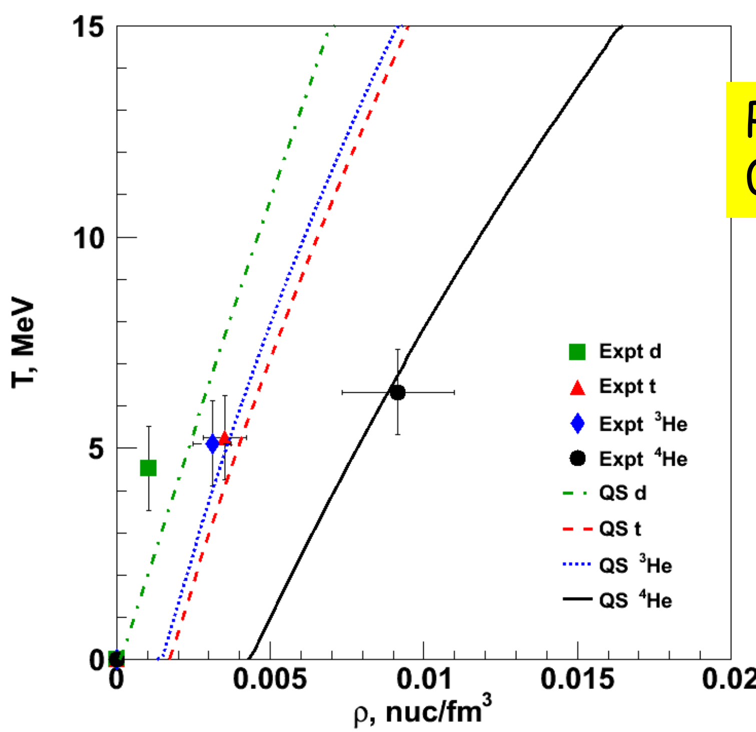

PRL **108** (2012) 062702

Temperatures and Densities

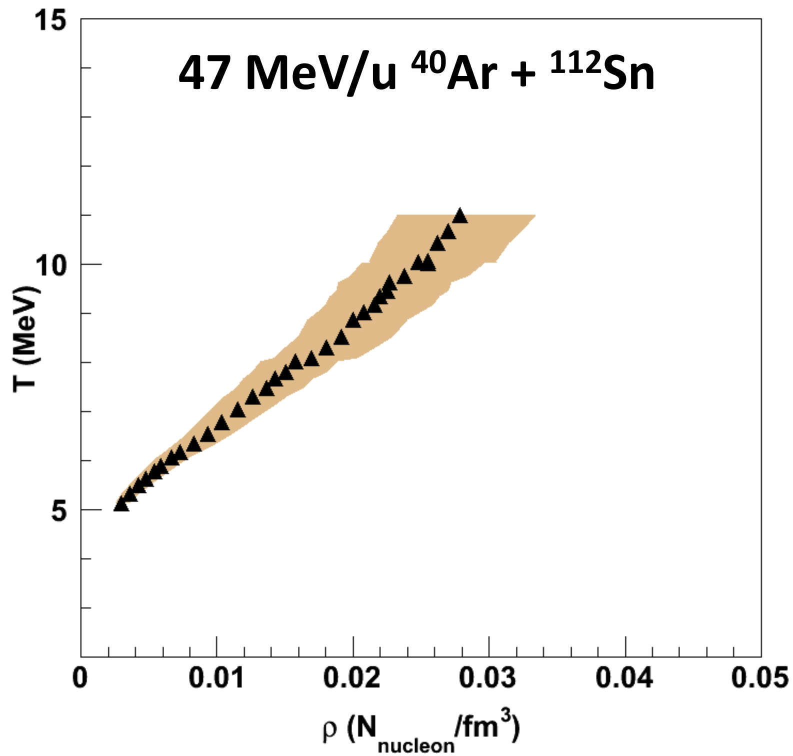

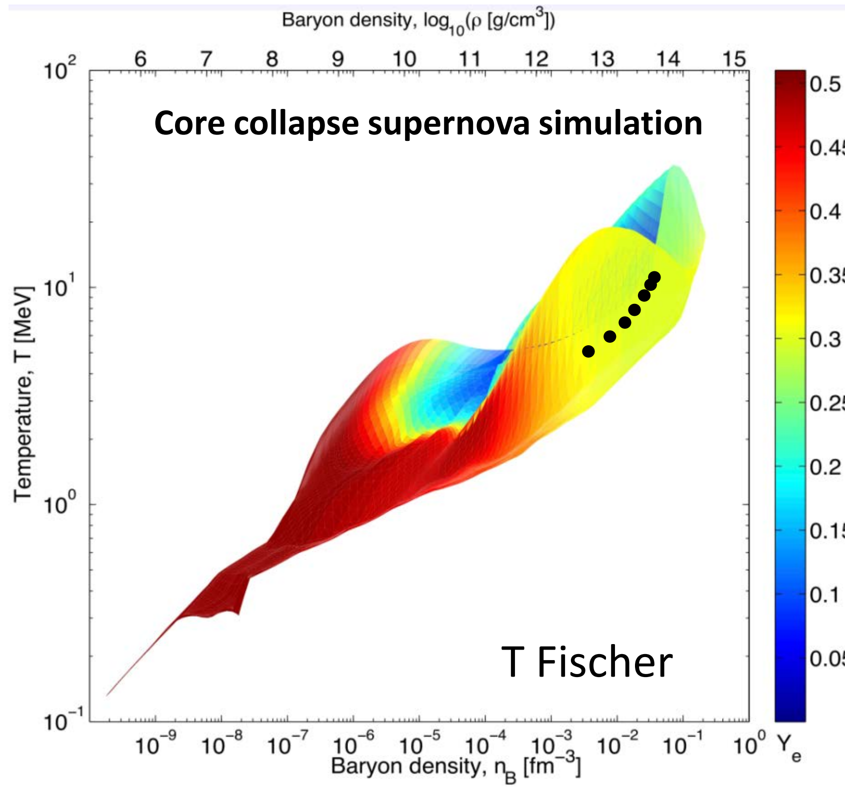

- Recall v_{surf} vs time calculation
- System starts hot
- As it cools, it expands

	Supernova	Heavy Ion Nuclear reaction
Density (nuc/fm^3)	$10^{-10} < \rho < 2$	$2\times10^{-3} < \rho < 3\times10^{-2}$
Temperature (MeV)	$\sim0 < T < 30$	$5 < T < 11$
Electron fraction	$0 < Y_p < 0.6$	$Y_p \sim 0.41$

Comparison of all models together

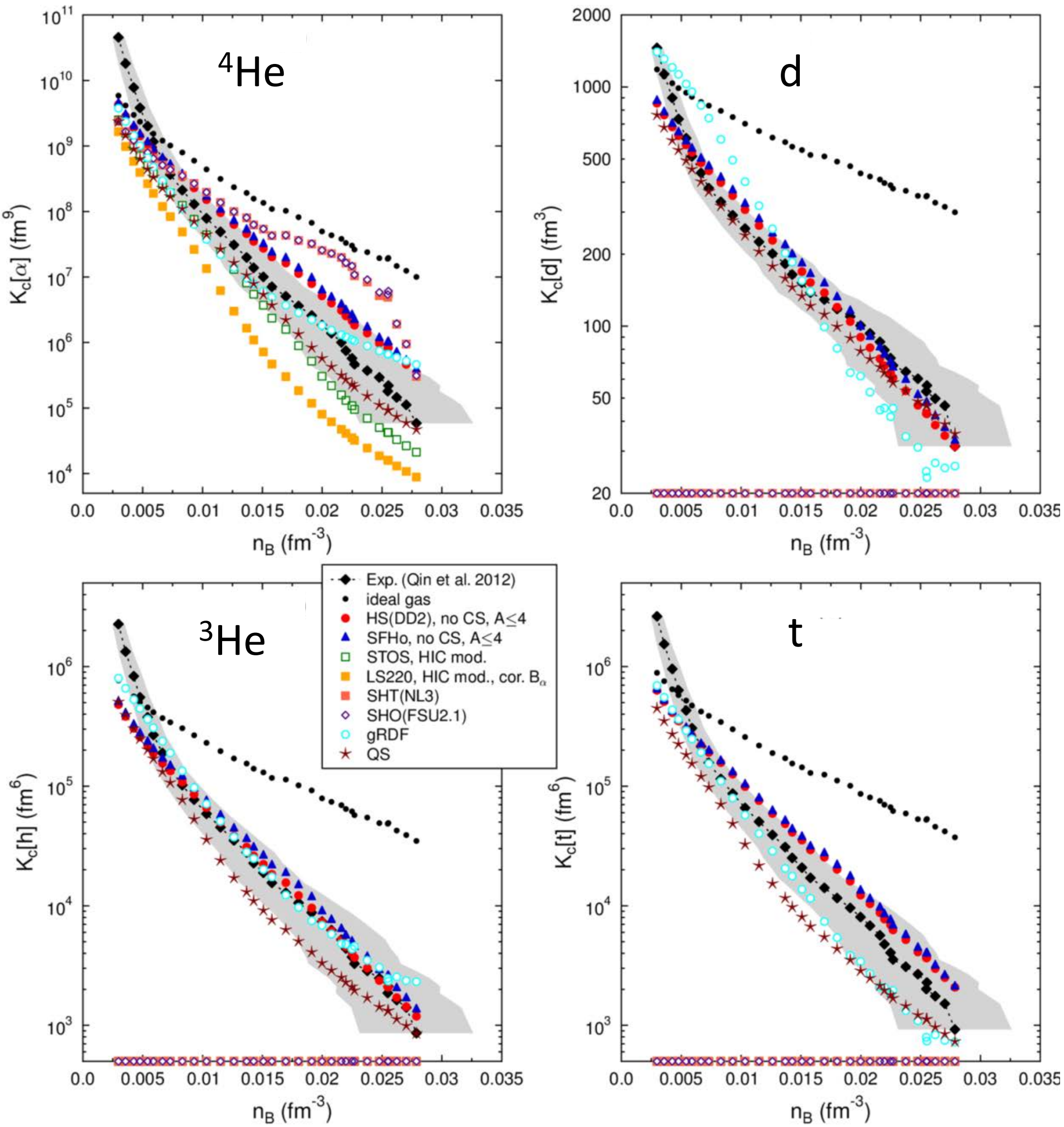

- Two groups of calculations
  - n, p, α calculations which predict $K_{eq}(\alpha)$, but cannot predict other species.
  - Models with n, p, d, t, ^{3}He, α
- Low densities
  - All $K_{eq}(\alpha)$ converge to ideal gas
  - They are below experimental data which result from the very late stages of the reaction
- Models that treat all light particles are generally within error bars

M. Hempel et al.
Phys. Rev. C **91**, 045805 (2015).

INDRA@GANIL experiment

32A MeV $^{136,124}Xe+^{124,112}Sn$

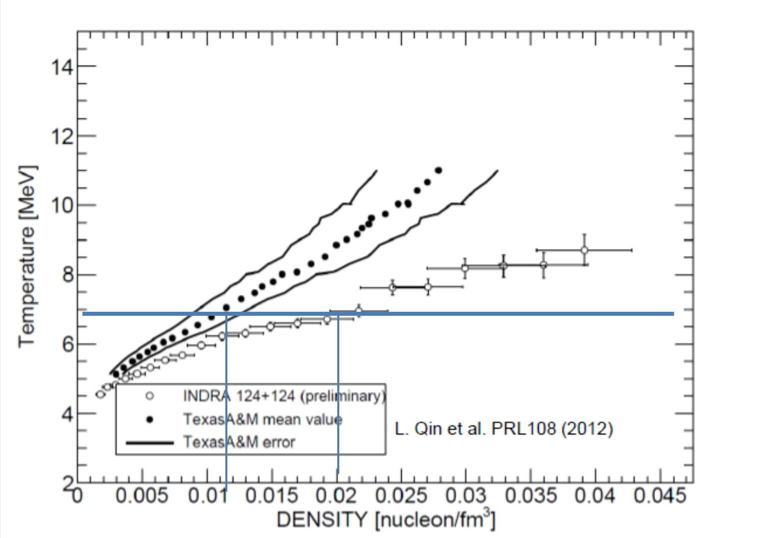

Remi Bougault
Private Communication
October 2018

The INDRA Collaboration

Texas A&M and INDRA data

EQUILIBRIUM CONSTANTS

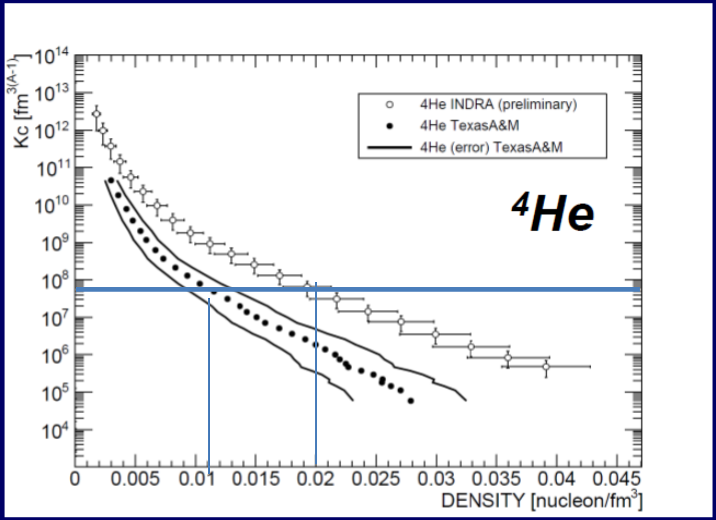

Different T-Rho Trajectory
At different denities but same T=7 MeV
Experimental KGanil= KTamu

PHYSICAL REVIEW C **97**, 045805 (2018)

Light clusters in warm stellar matter: Explicit mass shifts and universal cluster-meson couplings

Helena Pais,[1] Francesca Gulminelli,[2] Constança Providência,[1] and Gerd Röpke[3,4]
[1] *CFisUC, Department of Physics, University of Coimbra, 3004-516 Coimbra, Portugal*
[2] *LPC (CNRS/ENSICAEN/Université de Caen Normandie), UMR6534, 14050 Caen Cédex, France*
[3] *Institut für Physik, Universität Rostock, D-18051 Rostock, Germany*
[4] *National Research Nuclear University (MEPhI), 115409 Moscow, Russia*

(Received 15 January 2018; published 16 April 2018)

In-medium modifications of light cluster properties in warm stellar matter are studied within the relativistic mean-field approximation. In-medium effects are included by introducing an explicit binding energy shift analytically calculated in the Thomas-Fermi approximation, supplemented with a phenomenological modification of the cluster couplings to the σ meson. A linear dependence on the σ meson is assumed for the cluster mass, and the associated coupling constant is fixed by imposing that the virial limit at low density is recovered. The resulting cluster abundances come out to be in reasonable agreement with constraints at higher density coming from heavy-ion collision data. Some comparisons with microscopic calculations are also shown.

Texas A&M and Model

RMF MODEL (FSU) – different coupling constants

H. Pais, F. Gulminelli, C. Providencia, and G. Ropke Phys. Rev. C 97, 045805 (2018)

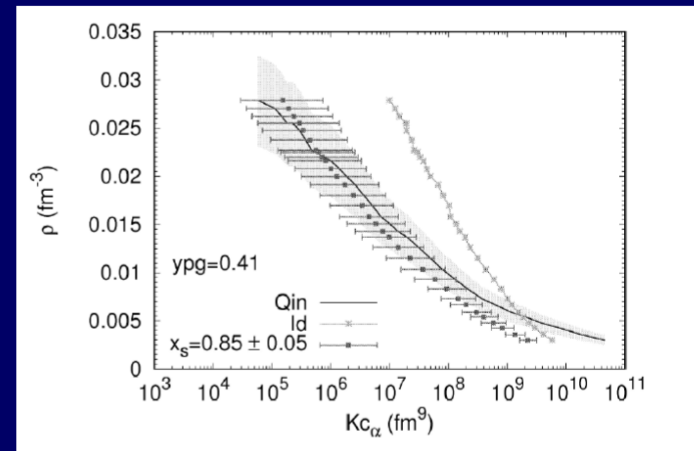

The other quantity that considers in-medium effects is the scalar cluster-meson coupling, $g_s^i = x_s^i A_i g_s$, which is determined from experimental constraints. We fix x_s^i so that in the low-density limit the virial EoS is reproduced. We obtained [20] $x_s^i = 0.85 \pm 0.05$ as good universal scalar cluster-meson coupling, that not only reproduces reasonably well the virial EoS but also reproduces well data coming from heavy-ion collisions in the high-density limit. We will consider this result for the cluster meson couplings throughout this paper.

RMF MODEL (FSU) – different coupling constants

H. Pais, F. Gulminelli, C. Providencia, and G. Ropke Phys. Rev. C **97**, 045805 (2018)

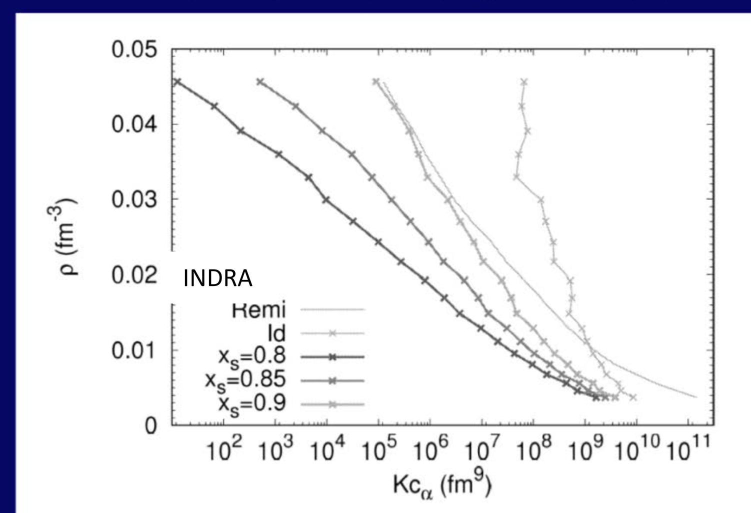

Full distribution of clusters with universal couplings and in-medium effects

Helena Pais,[1] Francesca Gulminelli,[2] Constança Providência,[1] and Gerd Röpke[3,4]
[1]CFisUC, Department of Physics, University of Coimbra, 3004-516 Coimbra, Portugal
[2]LPC (CNRS/ENSICAEN/Université de Caen Normandie), UMR6534, 14050 Caen cédex, France
[3]Institut für Physik, Universität Rostock, D-18051 Rostock, Germany
[4]National Research Nuclear University (MEPhI), 115409 Moscow, Russia

(Received 13 December 2018; published 10 May 2019)

Light and heavy clusters are calculated for asymmetric warm nuclear matter in a relativistic mean-field approach. In-medium effects, introduced via a universal cluster-meson coupling, and a binding energy shift contribution, calculated in a Thomas-Fermi approximation, were taken into account. This work considers, besides the standard lightest bound clusters ^{4}He, ^{3}He, ^{3}H, and ^{2}H, also stable and unstable clusters with higher number of nucleons, in the range $5 \leqslant A \leqslant 12$, as it is natural that heavier clusters also form in core-collapse supernova matter, before the pasta phases set in. We show that these extra degrees of freedom contribute with non-negligible mass fractions to the composition of nuclear matter, and may prevail over deuterons and α particles at high density in strongly asymmetric matter, and not too high temperatures. The presence of the light clusters reduces the contribution of heavy clusters to a much smaller density range, and to a smaller mass fraction.

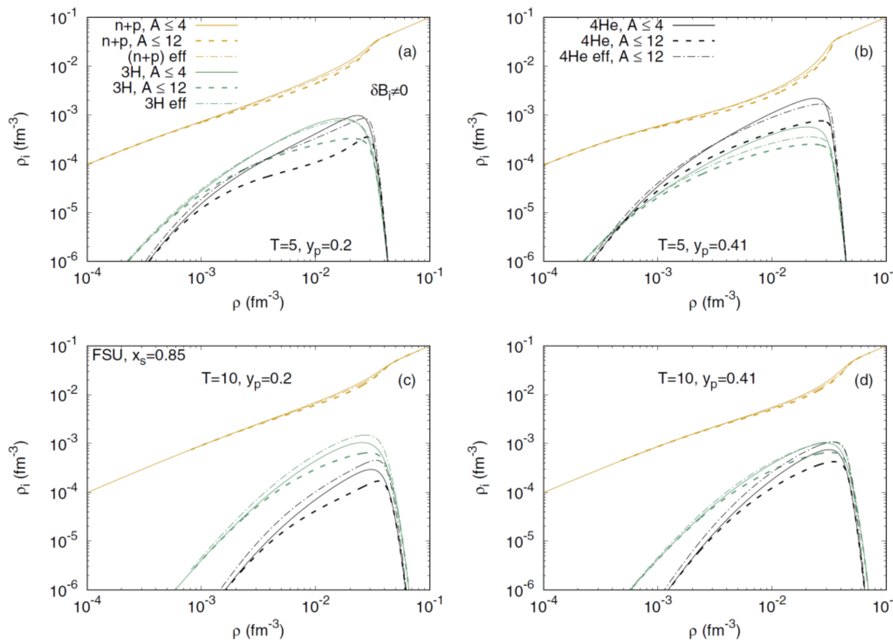

FIG. 6. Effective densities (dash-dotted lines) of free nucleons (orange), tritons (green), and α (black), compared to their primary (without the contribution of secondary decay, see text) densities (dashed lines) in a calculation with $A \leqslant 12$, as a function of the total density, considering $T = 5$ (top) and 10 MeV (bottom), and taking $y_p = 0.2$ (left) and 0.41 (right). A calculation with $A \leqslant 4$ is also shown (solid lines).

Equilibrium constants

Qin et al, PRL 108, 172701 2012

- Kc calculated with data from HIC:

$$K_c[j] = \frac{\rho_j}{\rho_n^{N_j}\,\rho_p^{Z_j}}$$

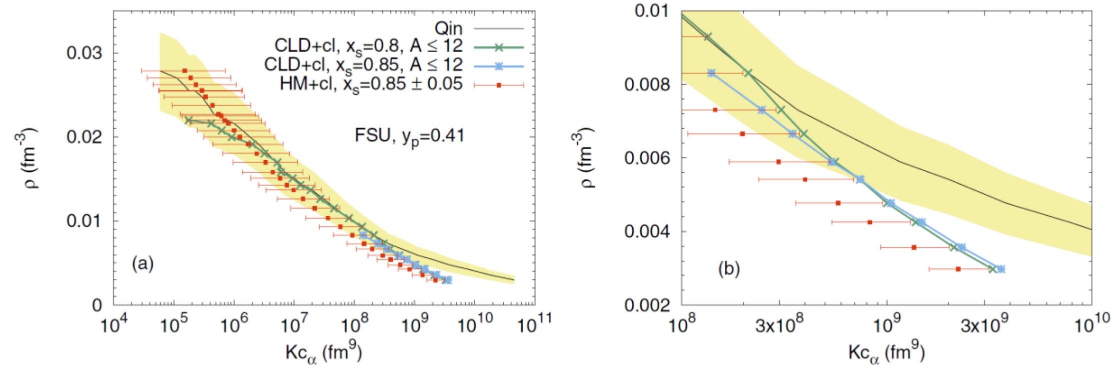

FIG. 14. Chemical equilibrium constants of α for FSU, and $y_p = 0.41$, and for the universal g_{s_j} fitting with $g_{s_j} = (0.85 \pm 0.05)A_j g_s$, considering a calculation with only the classical light clusters (red), and comparing with the CLD calculation with light clusters, taking $A \leqslant 12$, with the $x_s = 0.8$ (green) and $x_s = 0.85$ (cyan). The experimental results of Qin *et al.* [19] (solid black line and yellow uncertainty region) are also shown. The right panel shows in more detail the lowest density points of our calculations.

- Unique existing constraint on in-medium modifications of light clusters at finite T

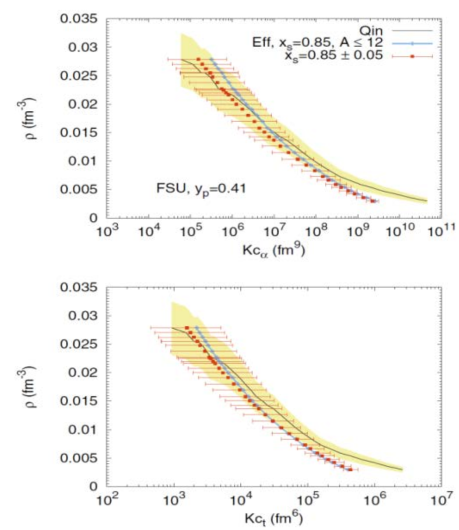

FIG. 7. Chemical equilibrium constants of α (top), and triton (bottom) for FSU, and $y_p = 0.41$, and for the universal $g_{s_j} = (0.85 \pm 0.05)A_j g_s$ fitting, from a calculation with only the four classical light clusters (red with arrow bars), and a calculation with $A \leqslant 12$, taking the effective densities, and $x_s = 0.85$ (cyan/gray thick line). The experimental results of Qin *et al.* [19] (yellow/gray shaded region) are also shown.

- Our model describes quite well exp data!

Helena Pais
CFisUC, University of Coimbra, Portugal

in collaboration with C. Providência, F. Gulminelli, and G. Roepke

International Workshop on Nuclear Dynamics in Heavy-Ion Reactions (IWND),
Huzhou, P.R. China, June 12th, 2018

Available online at www.sciencedirect.com
ScienceDirect
Nuclear Physics A 776 (2006) 55–79
NUCLEAR PHYSICS A

Cluster formation and the virial equation of state of low-density nuclear matter

C.J. Horowitz, A. Schwenk *
Nuclear Theory Center and Department of Physics, Indiana University, Bloomington, IN 47408, USA

Received 22 November 2005; received in revised form 1 February 2006; accepted 30 May 2006
Available online 7 July 2006

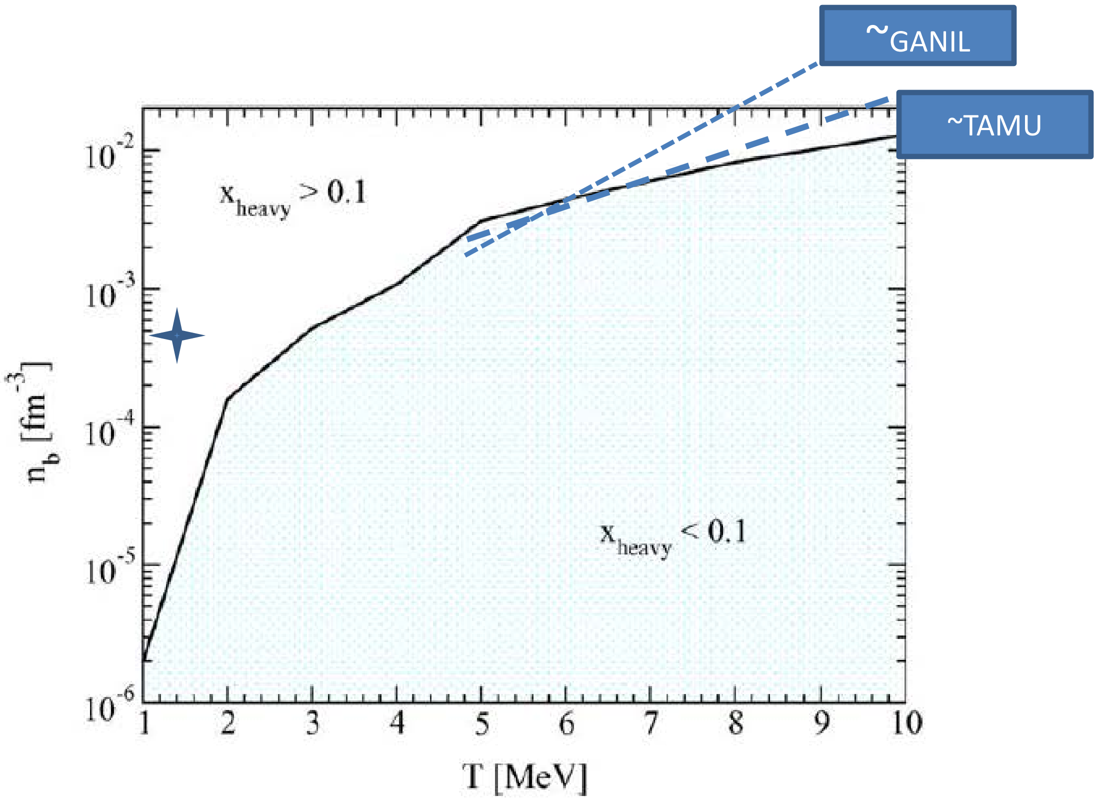

Fig. 9. (Color online.) The threshold baryon density n_b above which the Shen equation of state [27] predicts a heavy nuclei mass fraction larger than 10%. This figure is for $Y_p = 1/2$.

Light Particle Accompanied or “Ternary” Fission

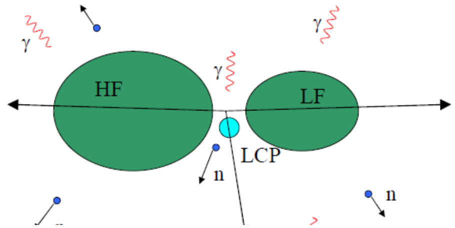

1. L. L. Green and D. L. Livesey, Nature **159**, 332 (1947).
2. S. T. Tsien et al., Nature **159**, 773 (1947).

I. Halpern, E. Henley
Alpha particle emission in fission, in *Physics and Chemistry of Fission* : CERN Report 1963 (unpublished); **Physics and Chemistry of Fission** (International Atomic Energy Agency, **Vienna**, **1965**) Vol.**2**(Vienna, 1965), p. 369

Fission Chips

Not long after the discovery of fission it was found that there is a small chance (~ 1/300) that the two fission fragments are accompanied by an alpha particle. A number of recent measurements[1–6] have given us further information on these emissions and have shown that sometimes other light nuclear particles can also be emitted in coincidence with fission fragments. The probabilities for these emissions are summarized in the Table and are even lower than those for α particles.

Probabilities for the emission of light charged particles in coincidence with fission fragments. The numbers given are very rough and apply to the spontaneous fission of ^{252}Cf.

$z = 1$	^{1}H	5×10^{-5}
	^{2}H	2×10^{-5}
	^{3}H	2×10^{-4}
$z = 2$	^{3}He	3×10^{-6}
	^{4}He	3×10^{-3}
	^{6}He	$(3–8) \times 10^{-5}$
	^{8}He	$(2–6) \times 10^{-6}$
$z = 3$	Li	4×10^{-6}
$z = 4$	Be	6×10^{-6}

Detection of Long-Range Fragments from Decay of Cf^{252}†

JOSEPH B. NATOWITZ,* ARASTOO KHODAI-JOOPARI,‡ AND JOHN M. ALEXANDER§
Department of Chemistry, State University of New York at Stony Brook, Stony Brook, New York

AND

T. DARRAH THOMAS§
Department of Chemistry, Princeton University, Princeton, New Jersey

(Received 12 January 1968)

Long-range products from the decay of Cf^{252} have been observed by range discrimination and detection of tracks in mica and lexan. Integrated yields (events per binary fission) of $\gtrsim 18\times10^{-6}$ and kinetic energies of 1.5–4 MeV/amu are indicated for fragments of B, C, N, and O. Integrated yields of $\gtrsim 3\times10^{-6}$ and kinetic energies of 1.5–2.5 MeV/amu are indicated for fragments of oxygen or heavier nuclei.

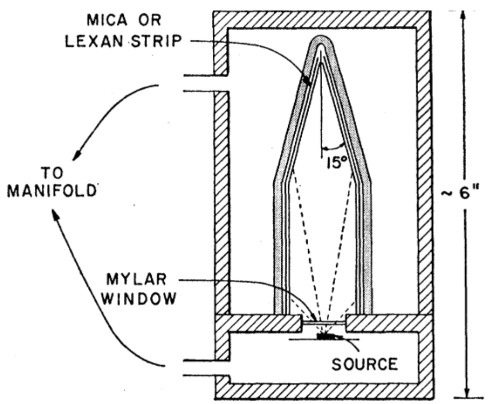

FIG. 1. Schematic diagram of the detection chamber. The Cf^{252} source was covered by a Ni foil of 0.52 mg/cm². Fragments impinged on the track detectors at angles of 40°–15°. The first 7 mm of the track detectors were shadowed from the source by the window mount.

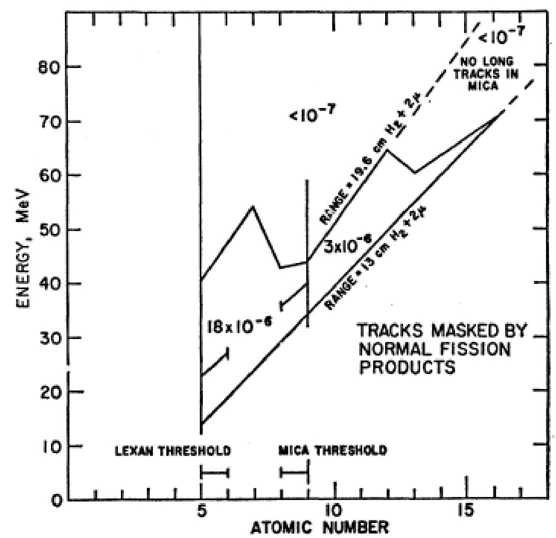

FIG. 5. Energy and atomic number limits for the long-range fragments as determined by ranges and registration properties. Yields are indicated for the energy-atomic number regions accessible in this study (see text).

Mica and lexan track detectors were employed to observe the yield (number of events per binary fission) of fragments emitted from ^{252}Cf as a function of range in H_2. These experiments were carried out in the chamber depicted in Fig. 1.

Light Particle Accompanied or “Ternary” Fission

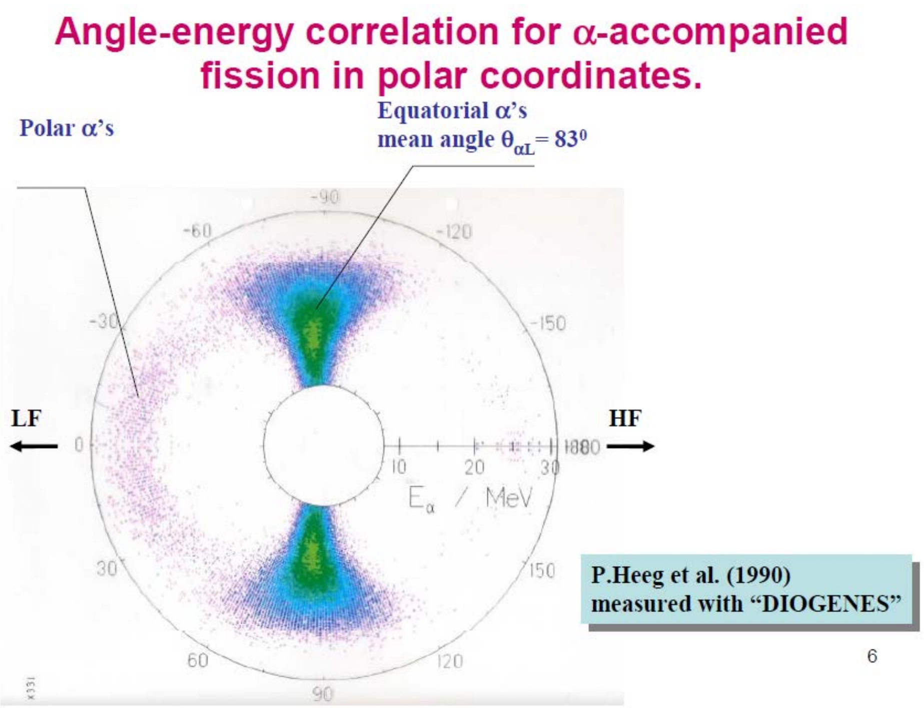

252 Cf - Thesis T U Darmstadt

- LCP’s are emitted nearly perpendicular to the fission axis
- > 90% of all ternary particles are α-particles
- Yields of heavier particles drastically decreases with the increase of LCP mass
- The energy distribution of LCP has nearly Gaussian shape with $\langle E_\alpha \rangle \approx 15$ MeV
- The emission of LCP slightly changes energy and mass distributions of fission fragments as well as other parameters, e.g. $\bar{\nu}$, M_γ etc.
- Ternary fission is a unique tool to study the energetics and dynamics of the fission process at scission.

IAEA-TECDOC-1168

XA0100142

Compilation and evaluation of fission yield nuclear data

Final report of a co-ordinated research project 1991–1996

TABLE 4.4.5. RECOMMENDED LIGHT CHARGED PARTICLE YIELDS FOR HYDROGEN ISOTOPES AND ^{4}HE RESULTING FROM ANALYSIS OF THE UKFY3 MEASUREMENT DATABASE.

Neutron energy	System	Mass	Yield per 100 fissions	Standard deviation (%)	Number of data points
Thermal	U233	1	6.542E-03	40.2	1
Thermal	U235	1	1.711E-03	10.8	3
Thermal	Pu239	1	4.080E-03	10.0	1
Fast	U235	1	1.174E-02	51.1	1
High	U233	1	9.018E-03	41.4	1
High	U235	1	6.335E-03	40.4	1
High	U238	1	2.001E-03	100.5	1
High	Np237	1	1.902E-02	41.4	1
Spontaneous	Cf252	1	6.086E-03	23.4	2
Spontaneous	Cf250	1	9.000E-03	25.0	1
Spontaneous	Fm256	1	7.000E-03	30.0	1
Spontaneous	Cm244	1	1.221E-02	41.0	1
Thermal	U233	2	8.466E-04	15.6	1
Thermal	U235	2	8.400E-04	17.9	2
Thermal	Pu239	2	1.347E-03	14.2	2
Spontaneous	Cf252	2	1.500E-03	20.0	1
Thermal	U233	3	9.691E-03	14.3	4
Thermal	U235	3	9.314E-03	3.8	15
Thermal	Pu239	3	1.442E-02	5.3	5
Thermal	Pu241	3	1.410E-02	10.0	1
Fast	U235	3	1.352E-02	11.7	4
Fast	Pu239	3	1.413E-02	15.9	1
High	U233	3	2.480E-02	22.6	1
High	U235	3	1.742E-02	20.7	1
High	U238	3	6.499E-03	22.1	1
High	Np237	3	3.329E-02	22.6	1
Spontaneous	Cf252	3	2.244E-02	3.9	8
Spontaneous	Cf250	3	2.700E-02	20.0	1
Spontaneous	Fm256	3	3.900E-02	15.0	1
Spontaneous	Cm244	3	2.197E-02	22.0	1
Thermal	U233	4	2.065E-01	4.1	9
Thermal	U235	4	1.699E-01	3.6	12
Thermal	Pu239	4	2.080E-01	3.3	8
Thermal	Pu241	4	2.015E-01	10.0	2
Fast	U233	4	2.003E-01	10.8	1
Fast	U235	4	1.980E-01	8.6	4
Fast	Pu239	4	2.029E-01	8.7	2
High	Th232	4	7.181E-02	36.4	2
High	U233	4	1.957E-01	10.6	1
High	U235	4	1.667E-01	5.3	3
High	U238	4	8.226E-02	9.5	4
High	Np237	4	2.010E-01	10.6	1
Spontaneous	Pu240	4	3.190E-01	10.0	1
Spontaneous	Pu242	4	2.740E-01	10.0	1
Spontaneous	Cf252	4	3.102E-01	6.3	4
Spontaneous	Cf250	4	3.980E-01	10.0	1
Spontaneous	Fm256	4	4.742E-01	8.3	2
Spontaneous	Fm257	4	3.994E-01	7.1	2
Spontaneous	Cm244	4	2.849E-01	9.1	3
Spontaneous	Cm242	4	3.601E-01	12.1	2

ELSEVIER

Nuclear Physics A 652 (1999) 371–387

NUCLEAR PHYSICS A

www.elsevier.nl/locate/npe

Ternary fission yields of ^{241}Pu(n_{th},f)

U. Köster [a,1], H.Faust [b], G. Fioni [c], T. Friedrichs [b,d], M. Groß [e], S. Oberstedt [b]

[a] *Technische Universität München, Physik-Department, 85748 Garching, Bavaria, Germany*
[b] *Institut Laue Langevin, 38042 Grenoble, France*
[c] *CEA Saclay, DSM/DAPNIA/SPHN, 91191 Gif-sur-Yvette, France*
[d] *Technische Universität Braunschweig, Institut für Metallphysik und Nukleare Festkörperphysik, 38106 Braunschweig, Germany*
[e] *Ludwig-Maximilians-Universität, Sektion für Physik, 85748 Garching, Bavaria, Germany*

Received 8 February 1999; revised 18 February 1999; accepted 23 February 1999

Abstract

Ternary events in the thermal neutron induced fission of ^{241}Pu(n,f) were studied with the recoil separator LOHENGRIN at the high-flux reactor of the Institut Laue Langevin in Grenoble. Yields and energy distributions could be determined for most isotopes of the elements hydrogen to oxygen. Also several heavier nuclei up to ^{30}Mg could be observed. Yields were measured for 42 isotopes, for further 17 isotopes upper limits could be deduced. For the first time the halo nuclei ^{11}Li, ^{14}Be and ^{19}C were found in neutron induced fission with yields of some 10^{-10} per fission.
© 1999 Elsevier Science B.V. All rights reserved.

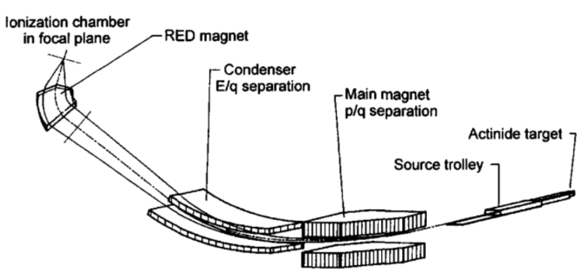

Fig. 1. Arrangement of the recoil separator LOHENGRIN.

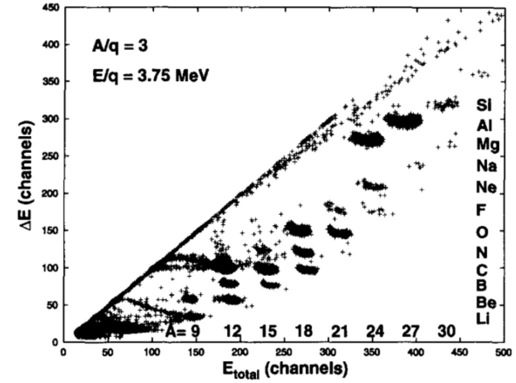

Fig. 3. ΔE–E scatter plot with separator setting $A/q = 3$ and $E/q = 3.75$ MeV. The measurement time for this spectrum was 6.1 h. The horizontal scale is proportional to the particle energy (and due to a fixed A/E ratio also to the mass), whereas the vertical scale is roughly proportional to the nuclear charge Z. Scattered binary particles create background close to the diagonal in the upper part of the spectrum. Background in the lower part is due to pile-up (from abundant ^{3}H and ^{6}He) and particles scattered in the entrance window of the ionization chamber (tails going to the top and left which can be seen at ^{6}He, ^{9}Li and ^{12}C). One channel corresponds approximately to 75 keV.

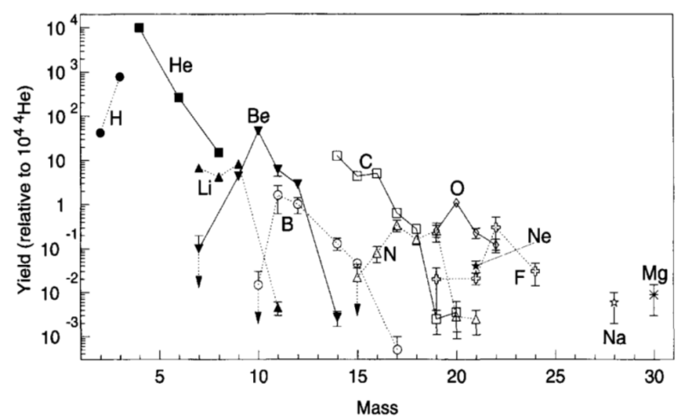

Fig. 7. Measured yields of ternary particles normalized to 10^4 for ^{4}He. The isotopes of each element are connected by a line, dashed for odd Z and solid for even Z. Upper limits are marked with an arrow. Some upper limits have been omitted for sake of clarity.

LA-UR-05-8860

An evaporation-based model of thermal neutron induced ternary fission of plutonium

J. P. Lestone,
Applied Physics Division, Los Alamos National Laboratory,
Los Alamos, New Mexico 87545, USA
(Received May 16th 2006)

Ternary fission probabilities for thermal neutron induced fission of plutonium are analyzed within the framework of an evaporation-based model where the complexity of time-varying potentials, associated with the neck collapse, are included in a simplistic fashion.

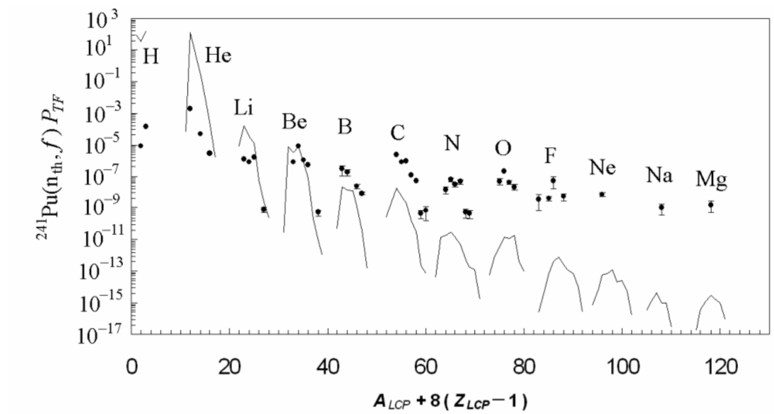

L

Fig. 6. Measured ternary fission emission probabilities for ^{241}Pu(n$_{th}$,f) [31]. The solid curves show a model calculation using static emission barriers with T_{scis}=1.1 MeV.

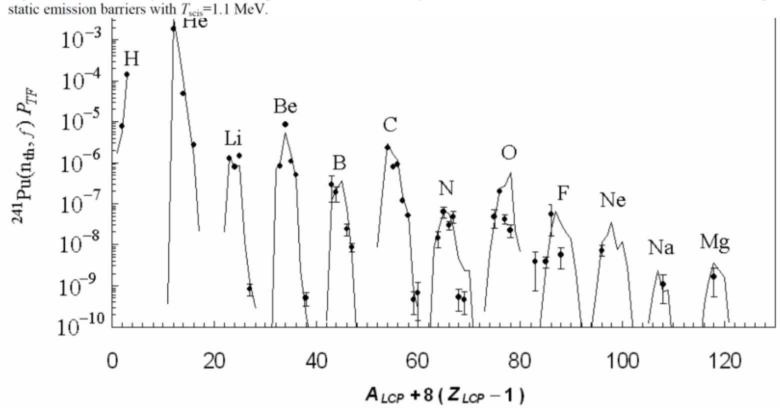

Fig. 7. Measured ternary fission emission probabilities for ^{241}Pu(n$_{th}$,f) [31]. The solid curves show a model calculation with T_{scis}=1.1 MeV, t_{NC}=1.6×10^{-22} s, and F_N=8.5 MeV/fm.

Is Cluster Formation in Low Density Skins the Explanation for
Light Particle Accompanied or “Ternary” Fission ?

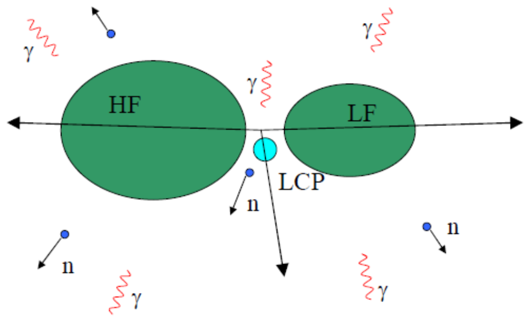

- LCP’s are emitted nearly perpendicular to the fission axis
- > 90% of all ternary particles are α-particles
- Yields of heavier particles drastically decreases with the increase of LCP mass
- The energy distribution of LCP has nearly Gaussian shape with $\langle E_\alpha \rangle \approx 15$ MeV
- The emission of LCP slightly changes energy and mass distributions of fission fragments as well as other parameters, e.g. $\bar{\nu}$, M_γ etc.
- Ternary fission is a unique tool to study the energetics and dynamics of the fission process at scission.

Angle-energy correlation for α-accompanied fission in polar coordinates.

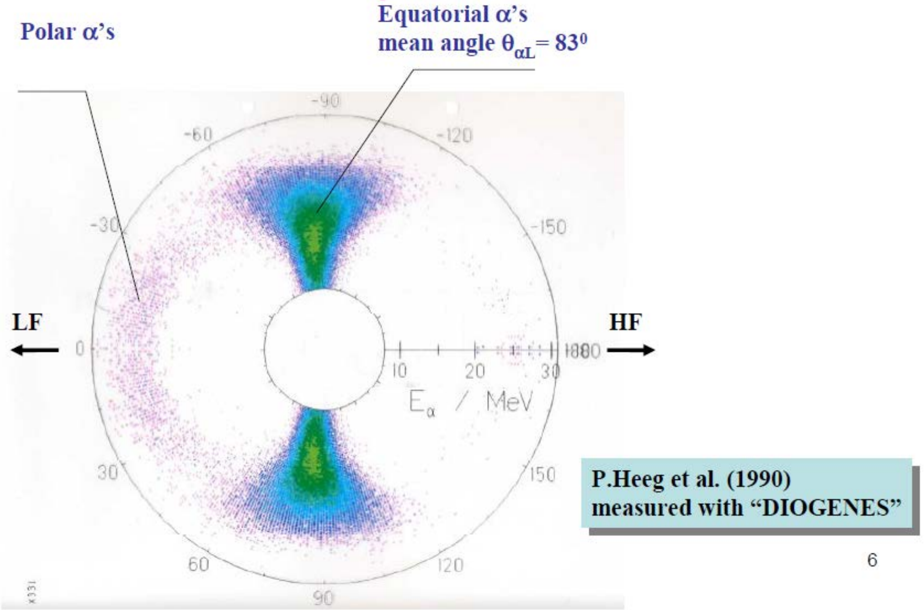

6

252 Cf - Thesis T U Darmstadt

Nucleation and cluster formation in low-density nucleonic matter: A mechanism for ternary fission

S. Wuenschel[1], H. Zheng[1], K. Hagel[1], B. Meyer[2], M. Barbui[1], E.J. Kim[1,3], G. Röpke[4] and J. B. Natowitz[1]
[1] *Cyclotron Institute, Texas A&M University, College Station, TX 77843, USA;*
[2] *Department of Physics and Astronomy, Clemson University, Clemson, SC 29634, USA;*
[3] *Division of Science Education, Chonbuk National University, Jeonju 561-756, Korea;*
[4] *University of Rostock, FB Physik, Rostock, Germany.*

Phys. Rev. C **90**, 011601(R) –
Published 8 July 2014

Ternary fission yields in the reaction ^{241}Pu(n_{th}, f) are calculated using a new model which assumes a nucleation-time moderated chemical equilibrium in the low density matter which constitutes the neck region of the scissioning system. The temperature, density, proton fraction and fission time required to fit the experimental data are derived and discussed. A reasonably good fit to the experimental data is obtained. This model provides a natural explanation for the observed yields of heavier isotopes relative to those of the lighter isotopes, the observation of low proton yields relative to ^{2}H and ^{3}H yields and the non-observation of ^{3}He, all features which are shared by similar thermal neutron induced and spontaneous fissioning systems.

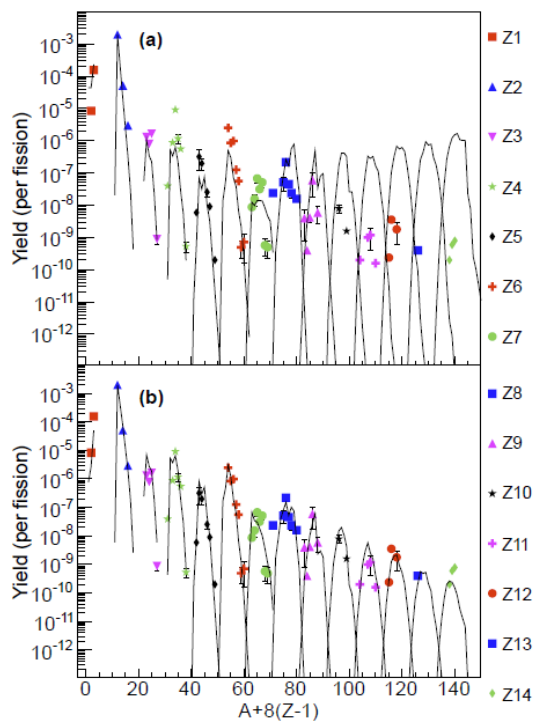

Figure 2: (Color online) Yield per fission as a function of mass(A) and charge(Z) of products. Solid points represent $^{241}Pu(n_{th}, f)$ experimental yields from Koester *et al* [9]. Lines are theoretical predictions from NSE calculation [7]. NSE parameters are $T = 1.4MeV$, $\rho = 4 \times 10^{-4} fm^{-3}$, and $Y_p = 0.34$. a) NSE calculation only. M^2 fit metric = 4.28. b) NSE calculation with nucleation. Nucleation parameters are time = $6400 fm/c$ and $A_c = 5.4$. Fit metric = 1.18.

Induced Fission of ^{240}Pu within a Real-Time Microscopic Framework

Aurel Bulgac,[1] Piotr Magierski,[1,2] Kenneth J. Roche,[1,3] and Ionel Stetcu[4]
[1]*Department of Physics, University of Washington, Seattle, Washington 98195-1560, USA*
[2]*Faculty of Physics, Warsaw University of Technology, ulica Koszykowa 75, 00-662 Warsaw, Poland*
[3]*Pacific Northwest National Laboratory, Richland, Washington 99352, USA*
[4]*Theoretical Division, Los Alamos National Laboratory, Los Alamos, New Mexico 87545, USA*
(Received 2 November 2015; revised manuscript received 18 January 2016; published 25 March 2016)

We describe the fissioning dynamics of ^{240}Pu from a configuration in the proximity of the outer fission barrier to full scission and the formation of the fragments within an implementation of density functional theory extended to superfluid systems and real-time dynamics. The fission fragments emerge with properties similar to those determined experimentally, while the fission dynamics appears to be quite complex, with many excited shape and pairing modes. The evolution is found to be much slower than previously expected, and the ultimate role of the collective inertia is found to be negligible in this fully nonadiabatic treatment of nuclear dynamics, where all collective degrees of freedom (CDOF) are included (unlike adiabatic treatments with a small number of CDOF).

TABLE I. The simulation number, the pairing parameter η, the excitation energy (E^*) of $^{240}_{94}$Pu$_{146}$ and of the f $[E^*_{H,L} = E_{H,L}(t_{SS}) - E_{gs}(N_{H,L}, Z_{H,L})]$, the equivalent neutron incident energy (E_n), the scaled initial mass moments q the "saddle-to-scission" time t_{SS}, TKE evaluated as in Ref. [71], TKE, atomic ($A_L^{\rm syst}$), neutron ($N_L^{\rm syst}$), and proton ($Z_L^{\rm sys}$ data [72] using Wahl's charge systematics [73] and the corresponding numbers obtained in simulations, and the numb neutrons for the heavy and light fragments ($\nu_{H,L}$), estimated using a Hauser-Feshbach approach and experimental n energies [8,74,75]. Units are in MeV, fm^2, fm^3, fm/c as appropriate.

S no.	η	E^*	E_n	q_{zz}	q_{zzz}	t_{SS}	TKE$^{\rm syst}$	TKE	$A_L^{\rm syst}$	A_L	$N_L^{\rm syst}$	N_L	$Z_L^{\rm syst}$	Z_L	E^*_H
$S1$	0.75	8.05	1.52	1.78	−0.742	14 419	177.27	182	100.55	104.0	61.10	62.8	39.45	41.2	5.26
$S2$	0.5	7.91	1.38	1.78	−0.737	4360	177.32	183	100.56	106.3	60.78	64.0	39.78	42.3	9.94
$S3$	0	8.08	1.55	1.78	−0.737	14 010	177.26	180	100.55	105.5	60.69	63.6	39.81	41.9	3.35
$S4$	0	6.17	−0.36	2.05	−0.956	12 751	177.92	181		103.9		62.6		41.3	7.85

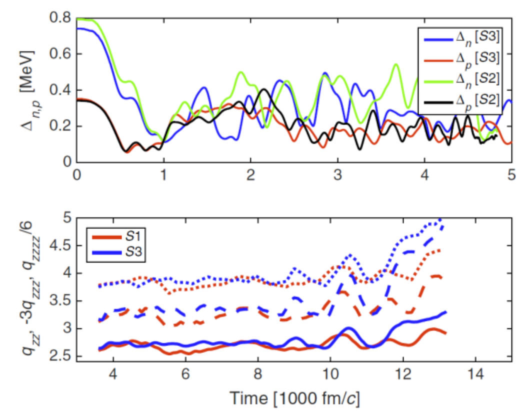

FIG. 2. The time dependence of spatially averaged $|\Delta_{n,p}(\mathbf{r},\mathbf{t})|$ for $S2$ (mixed pairing) and $S3$ (volume pairing) in the upper panel and, in the lower panel, the scaled mass moments $q_{20}(t) = \int d^3(3z^2 - r^2)/A^{5/3}\rho(\mathbf{r},t)$, $q_{30}(t) = \int d^3z(5z^2 - 3r^2)\rho(\mathbf{r},t)/A^2$, $q_{40}(t) = \int d^3(35z^4 - 30z^2r^2 + 3r^4)\rho(\mathbf{r},t)/A^{7/3}$, with solid, dotted, and dashed lines, respectively, for $S1$ (red) and $S3$ (blue) [fm^L]; see Table I.

Some Representative Publications of the VAST Literature on Ternary Fission

- F. Gonnenwein
- M. Mutterer
- C. Wagemans
- A. Yorobyev

And collaborators

Ternary and quaternary fission

Friedrich Gönnenwein[1], *Manfred Mutterer*[2] *and Yuri Kopatch*[3]
[1] *Physikalisches Institut, Universität Tübingen, Germany*
[2] *Institut für Kernphysik, Technische Universität Darmstadt, Germany*
[3] *Frank Laboratory of Neutron Physics, JINR, Dubna, Russia*

europhysics news JANUARY/FEBRUARY 2005

5He, 7He, and 8Li (E*=2.26MeV) intermediate ternary particles in the spontaneous fission of 252Cf

Yu. N. Kopatch, M. Mutterer, D. Schwalm, P. Thirolf, and F. Gönnenwein
Phys. Rev. C 65, 044614 – Published 1 April 2002

Energy distribution of ternary α particles in spontaneous fission of 252Cf

M. Mutterer, Yu. N. Kopatch, S. R. Yamaledtinov, V. G. Lyapin, J. von Kalben, S. V. Khlebnikov, M. Sillanpää, G. P. Tyurin, and W. H. Trzaska
Phys. Rev. C 78, 064616 – Published 30 December 2008

ELSEVIER
Available online at www.sciencedirect.com
SCIENCE DIRECT
Nuclear Physics A 742 (2004) 291–302
NUCLEAR PHYSICS A
www.elsevier.com/locate/npe

Energy distribution of the ternary alpha's emitted in ^{235}U(n_{th}, f) and ^{252}Cf(SF)

C. Wagemans [a,*], J. Heyse [b], P. Janssens [a], O. Serot [c], P. Geltenbort [d]

ISSN 1063-7761, Journal of Experimental and Theoretical Physics, 2018, Vol. 127, No. 4, pp. 659–670. © Pleiades Publishing, Inc., 2018.
Original Russian Text © A.S. Vorobyev, O.A. Shcherbakov, A.M. Gagarski, G.A. Petrov, G.V. Val'ski, T.E. Kuz'mina, 2018, published in Zhurnal Eksperimental'noi i Teoreticheskoi Fiziki, 2018, Vol. 154, No. 4, pp. 774–786.

NUCLEI, PARTICLES, FIELDS, GRAVITATION, AND ASTROPHYSICS

Estimation of the Yield of "Scission" Neutrons from Thermal Neutron-Induced Fission of ^{239}Pu

A. S. Vorobyev[a,*], O. A. Shcherbakov[a], A. M. Gagarski[a], G. A. Petrov[a], G. V. Val'ski[a], and T. E. Kuz'mina[b]

And references therein !

Experimental Determination of $K_{EQ}(\alpha)$

From the relevant literature

Particle	Total Yield/fission	Equatorial Emission	Adopted Value
n	2.95	0.104	0.104
p	4.08×10^{-5}	3.48×10^{-5}	3.48×10^{-5}
4He	2.07×10^{-3}	2.06×10^{-3}	1.72×10^{-3} (a)

(a) ^{5}He decay contribution removed

Coalescence Model Volume Calculation - (Mekjian Model) - 2822 fm^3

Particle Densities	K_{EXPT}
Rho n 3.70E-05	**3.01E+18**
Rho p 1.21E-08	
Rho α 6.09E-07	

NSE K_{EQ}	**4.86E+18**
PAIS K_{EQ} (FSU,.85)	**3.04E+18**

Evidence of a medium Effect?

ISSN 1063-7761, Journal of Experimental and Theoretical Physics, 2018, Vol. 127, No. 4, pp. 659–670. © Pleiades Publishing, Inc., 2018.
Original Russian Text © A.S. Vorobyev, O.A. Shcherbakov, A.M. Gagarski, G.A. Petrov, G.V. Val'ski, T.E. Kuz'mina, 2018, published in Zhurnal Eksperimental'noi i Teoreticheskoi Fiziki, 2018, Vol. 154, No. 4, pp. 774–786.

NUCLEI, PARTICLES, FIELDS, GRAVITATION, AND ASTROPHYSICS

Estimation of the Yield of "Scission" Neutrons from Thermal Neutron-Induced Fission of ^{239}Pu

A. S. Vorobyev[a,*], O. A. Shcherbakov[a], A. M. Gagarski[a], G. A. Petrov[a], G. V. Val'ski[a], and T. E. Kuz'mina[b]

[a] Petersburg Nuclear Physics Institute, National Research Centre "Kurchatov Institute," Gatchina, Leningrad oblast, 188300 Russia

[b] Khlopin Radium Institute, Rosatom State Atomic Energy Corporation, St. Petersburg, 194021 Russia

*e-mail: vorobyev_as@pnpi.nrcki.ru

Received April 26, 2018

The integral spectrum of PFNs calculated assuming the emission of neutrons only from fully accelerated fragments coincides with the measured spectrum to within errors of experimental data in the range of neutron energies 0.6–10 MeV, and the obtained average total number of PFNs per fission event (2.85 ± 0.03) is close to the recommended value of 2.8840 ± 0.0050 [4]. The average numbers of neutrons emitted from the light and heavy fragments amount to 1.62 ± 0.02 and 1.23 ± 0.02, respectively. The average energies of fission neutrons in the center-of-mass system of light and heavy fragment, as estimated from approximation of their spectra by a function of type (10), amount to 1.28 ± 0.02 MeV and 1.35 ± 0.02 MeV, respectively.

The percentage yield of scission neutrons relative to the total number ν_0 of PFNs per fission event and their average energy $\langle E_s \rangle = 2T_s$ determined in this way amounted to 3.6 ± 0.5% and 0.91 ± 0.19 MeV, respectively.

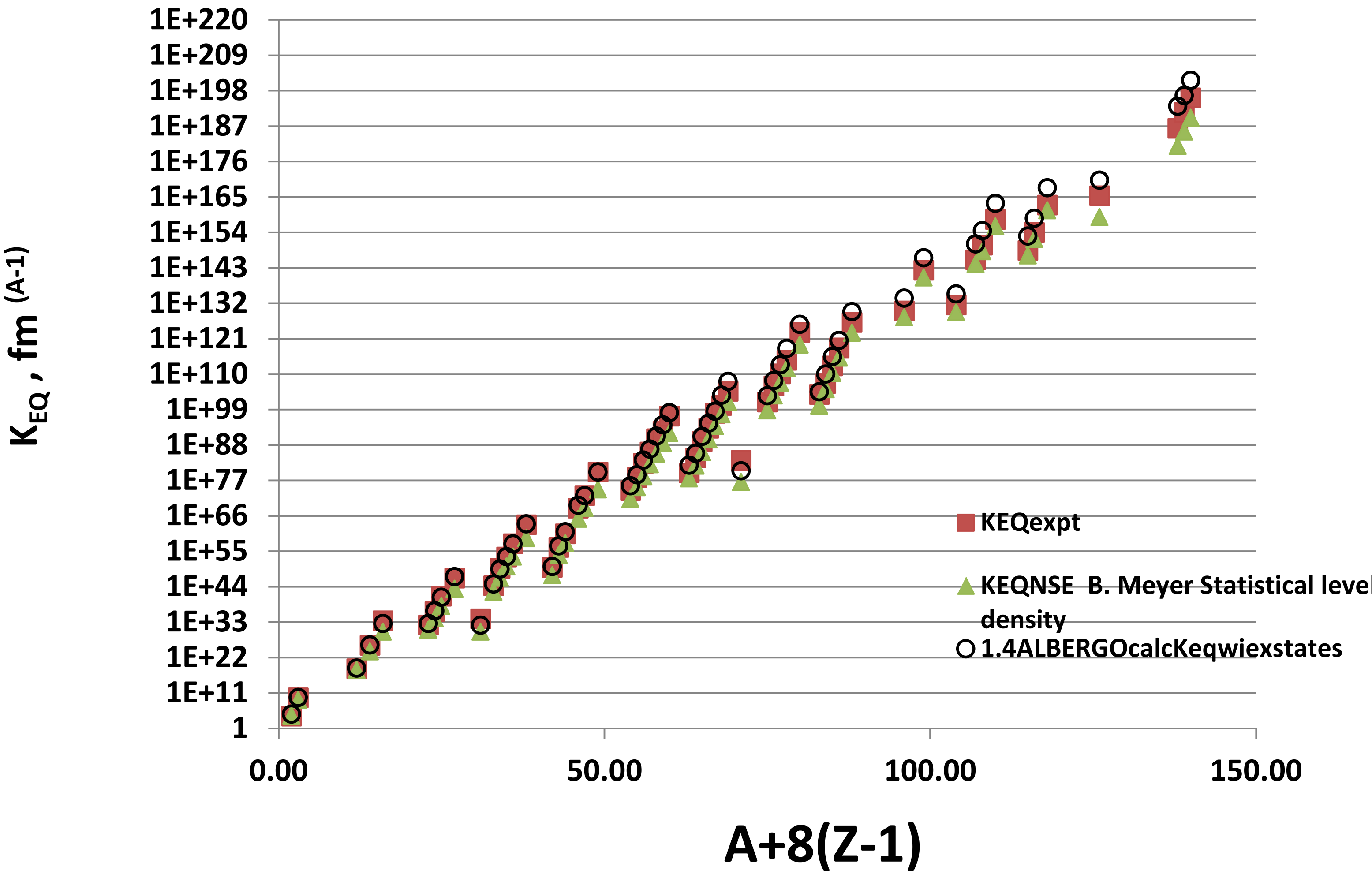
1E+220
1E+209
1E+198
1E+187
1E+176
1E+165
1E+154
1E+143
1E+132
1E+121
1E+110
1E+99
1E+88
1E+77
1E+66
1E+55
1E+44
1E+33
1E+22
1E+11
1
0.00
50.00
100.00
150.00
A+8(Z-1)
K_{EQ} , fm $^{(A-1)}$
KEQexpt
KEQNSE B. Meyer Statistical level density
1.4ALBERGOcalcKeqwiexstates

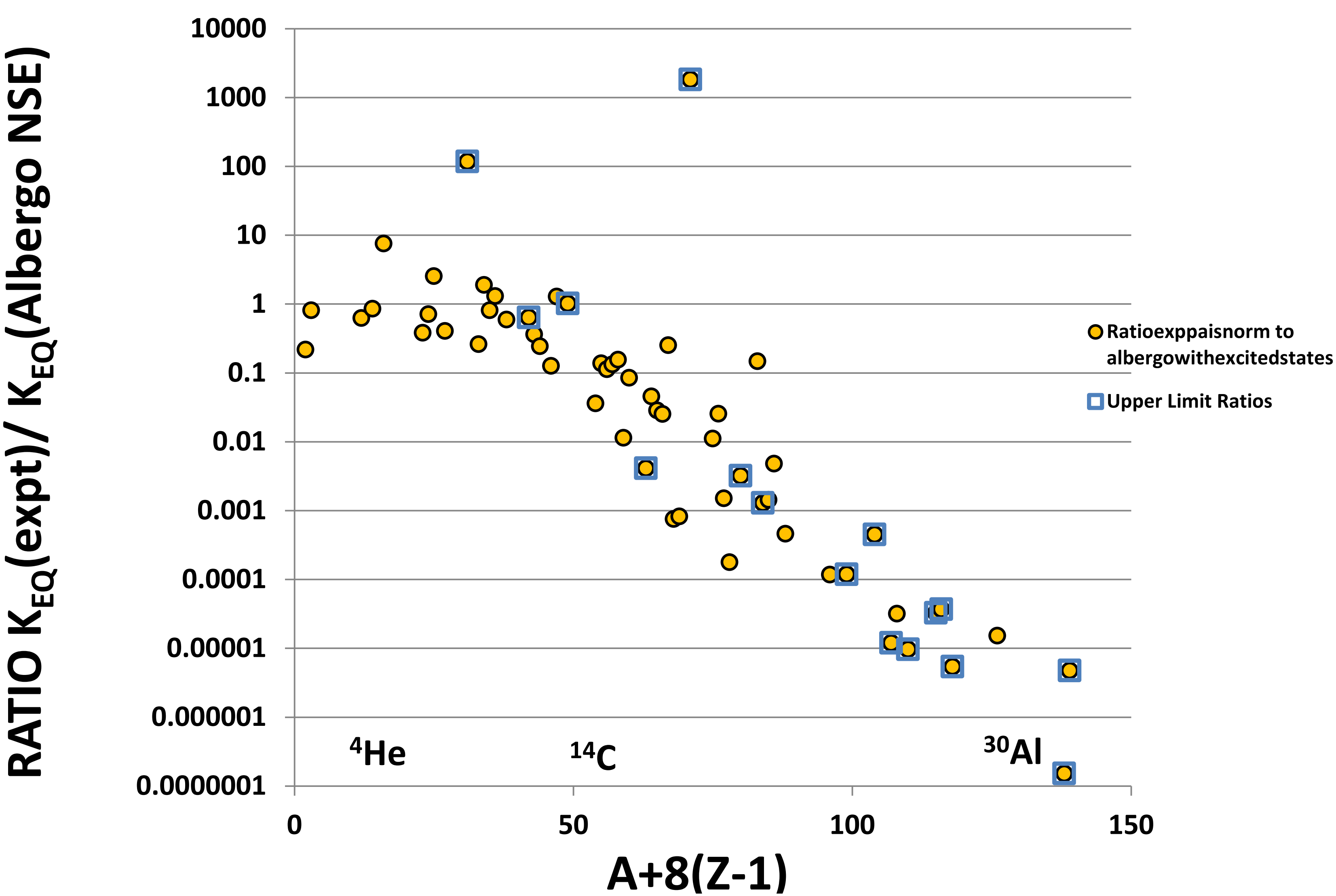

RATIO K_{EQ}(expt)/ K_{EQ}(Albergo NSE)
10000
1000
100
10
1
0.1
0.01
0.001
0.0001
0.00001
0.000001
0.0000001
0
50
100
150
A+8(Z-1)
^{4}He
^{14}C
^{30}Al
Ratioexppaisnorm to albergowithexcitedstates
Upper Limit Ratios

Summarizing Ternary Fission Analysis

Apparent equilibrium constants have been derived at $T=1.4$ MeV, $\rho= 4x\ 10^{-4}$ nuc /fm^3

Results indicate equilibrium achieved for $A \leq 14$
(for a relatively slow dynamic evolution)

Further theoretical analyses are underway

Role of medium effects, time restrictions, finite size effects all under investigation

Collaborators

K. Hagel, R. Wada, S. Kowalski, L. Qin, S. Wuenschel, M. Barbui, J. Gauthier, K. Schmidt, E. J. X. Cao, Kim,G. Röpke, M. Hempel, S. Typel, H.Pais, G. Giuliani, S. Shlomo, A. Bonasera, Z. Chen, M. Huang, J. Wang, H. Zheng, M. R. D. Rodrigues, D. Fabris, M. Lunardon, S. Moretto, G. Nebbia, S. Pesente, V. Rizzi, G. Viesti, M. Cinausero, G. Prete, T. Keutgen, Y. El Masri, Z. Majka, Y. G. Ma and J. B. Natowitz,

Texas A&M University, College Station, Texas
INFN Laboratori Nazionali di Legnaro, Legnaro, Italy
INFN Dipartimento di Fisica, Padova, Italy
Jagellonian University, Krakow, Poland
Silesian University, Katowice, Poland
Universität Darmstadt, Darmstadt, Germany
University of Rostock, Rostock, Germany
Basel University, Basel, Switzerland
UCL, Louvain-la-Neuve, Belgium
Shanghai Institute of Nuclear and Applied Physics, Shanghai, China
University of Coimbra, Coimbra, Portugal